Supporting information for the article:

Impact of a model soil microorganism and of its secretome on the fate of silver nanoparticles

Eymard-Vernain Elise , Lelong Cécile, Pradas del Real Ana-Elena, Soulas Romain, Bureau Sarah, Tardillo Suarez Vanessa, Gallet Benoit, Proux Olivier, Castillo-Michel Hiram and Sarret Géraldine

Environmental Science & Technology

This document contains 10 pages, with 11 Figures.

Materials and Methods

Nanoparticles

Ag_2S-NPs were obtained by sulfidation of PVP-Ag-NPs as described in Levard et al. (2011). Briefly, a suspension of 1mM PVP-Ag-NPs (pH=7) was mixed with a 1mM Na2S in a 0.01M NaNO3 electrolyte. After 7 days of agitation in open bottles, the suspension was centrifuged, washed three times with MQ water and dried. The total transformation of Ag0 to Ag2S was checked by X- ray diffraction (Figure S1).

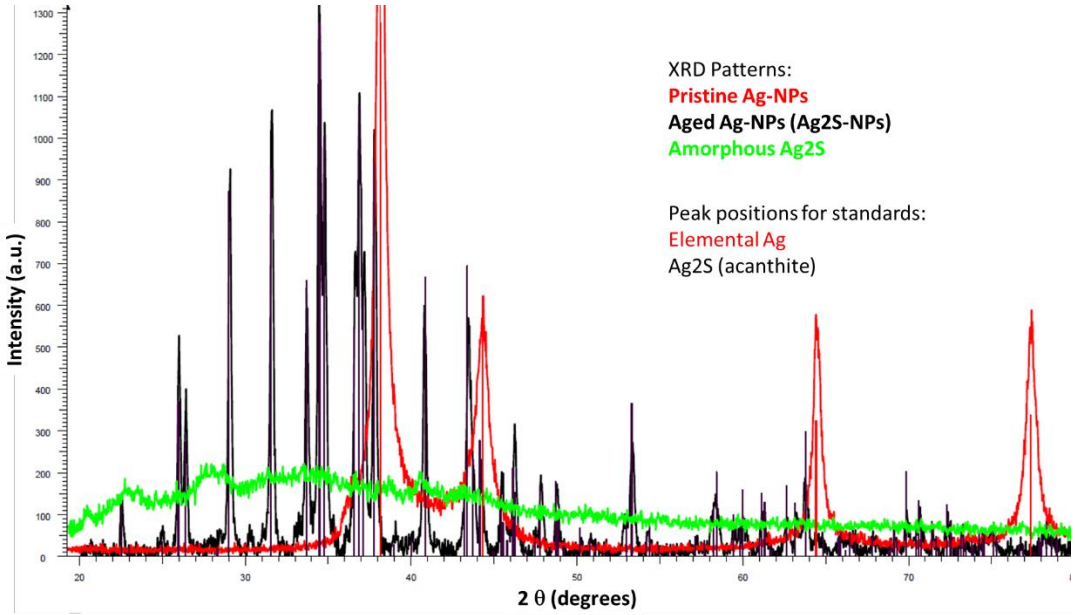

Figure S1: XRD analysis of the pristine Ag-NPs, and sulfidized Ag-NPs (Ag2S-NPs) and amorphous Ag2S. X-ray diffraction patterns (XRD) were recorded on powders using a D8 Bruker X-ray diffractometer and the CuKa radiation.

The zeta potential was measured for Ag-NPs and Ag2S-NPS over a range of pH from 4 to 9 (Figure S2). Aqueous solutions containing 1 g L^{-1} Ag-NPs, or 1g L^{-1} Ag_2S-NPs in 5 g L^{-1} NaCl were prepared at different pH values ranging from 6 to 10 for ζ potential measurements. NaOH and HCl were used to adjust the pH to the desired value. After dispersion, their zeta potential were measured using a Zetasizer Nano ZS Malvern Instruments. Three replicates of each sample were run for statistical purposes.

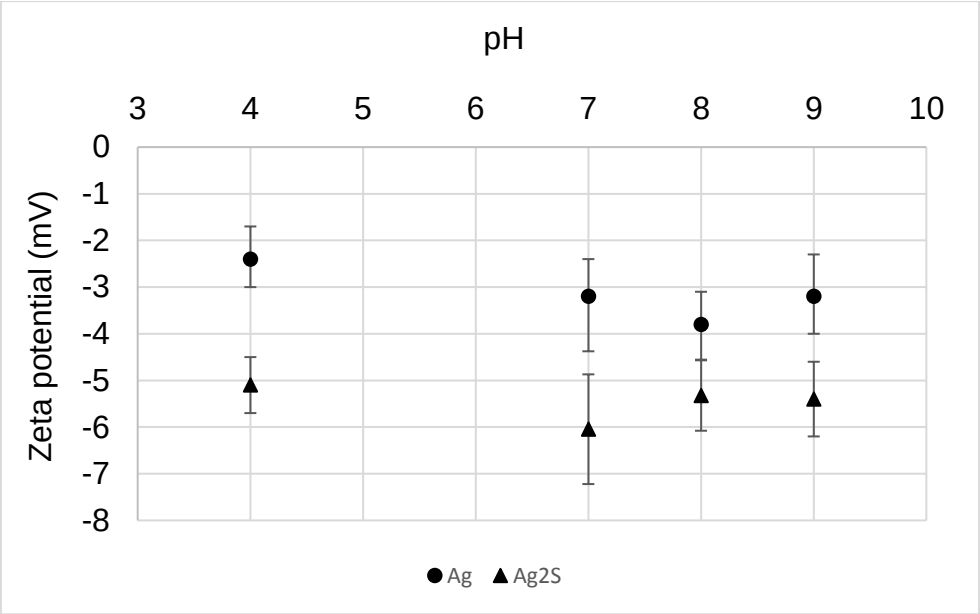

Figure S2: Zeta potential measured for the Ag-NPs and Ag_2S-NPs at various pHs.

High pressure freezing and freeze-substitution

Cells were centrifuged at 4500 g for 5 min. A pellet volume of 1.4 µl was dispensed on the 200-µm side of a type A 3-mm gold platelet (Leica Microsystems), covered with the flat side of a type B 3-mm aluminum platelet (Leica Microsystems), and was vitrified by high-pressure freezing using an HPM100 system (Leica Microsystems). Next, the samples were freeze substituted at −90°C for 80 h in acetone supplemented with 1% OsO4 and warmed up slowly (1°C/h) to −60°C in an automated freeze substitution device (AFS2; Leica Microsystems). After 8 to 12 h, the temperature was raised (1°C/h) to −30°C, and the samples were kept at this temperature for another 8 to 12 h before a step for 1h at 0°C, cooled down to 30°C and then rinsed 4 times in pure acetone. The samples were then infiltrated with gradually increasing concentrations of Agar Low Viscosity Resin (LVR; Agar Scientific) in acetone (1:2, 1:1, 2:1 [vol/vol], and pure) for 2 to 3 h while raising the temperature to 20°C. Pure LVR was added at room temperature. After polymerization 24h at 60°C, 70 to 400-nm sections were obtained using an ultra-microtome UC7 (Leica Microsystems) and an Ultra 35° diamond knife (DiATOME) and were collected on formvar-carbon-coated 100-mesh copper grids (for TEM) or on grids with a Si3N4 window (for nanoXRF/nanoXANES). The sections for TEM imaging were post-stained: 10 min with 2% aqueous uranyl acetate, rinsed, and incubated for 5 min with lead citrate.

Ag reference compounds for XAS analyses

For Ag K-edge XANES and EXAFS spectra recorded at 15°K, the following reference spectra were used. Solid state compounds, diluted in BN, included Ag^0 foil, Ag^0 nanoparticles (Ag-NPs), $AgPO_4$, AgCl, $AgNO_3$, Ag_2O, Ag_2CO_3, Ag diethyldithiocarbamate ($C_5H_{10}AgNS_2$, Ag-DEDTC), natural macrocrystalline Ag_2S (acanthite), Ag_2S-NPs obtained from the sulfidation of the Ag-NPs, and amorphous Ag2S obtained following the protocole described by Du et al. (2007). The complete sulfidation, from Ag^0 for the Ag-NPs to Ag2S-NPs, and the amorphous character of the amorphous Ag2S were verified by X- ray diffraction (XRD) (Figure S1). Ag compounds in solution included Ag^+ (25 mM AgNO3, pH 4.0), Ag malate (10 mM Ag, 100 mM malate, pH 5), Ag lactate (10 mM Ag lactate from sigma used for the exposure experiments, pH 5), and various Ag-GSH solutions prepared in anoxia described in Pradas del Real et al. (2016). Solution samples were mixed with 20-30% glycerol to prevent ice crystal formation during cooling.

For Ag K-edge nanoXANES spectra recorded at room temperature in full XAS mapping mode with an energy step of 5 eV below and above the edge (25.44 to 25.49 and 25.58 to 25.70 keV), and 1 eV in the edge (25.49 to 25.58 keV). Only two references spectra including Ag-NPs and Ag_2S-NPs were recorded, due to the limited beamtime. For Ag L-edge XANES spectra recorded at 80°K, the following reference spectra were used. Solid state compounds included Ag^0 foil, Ag^0 nanoparticles (Ag-NPs), Ag_2S-NPs AgCl, $AgNO_3$, Ag phosphate (Ag_3PO_4), Ag_2CO_3 and Ag diethyldithiocarbamate ($C_5H_{10}AgNS_2$, Ag-DEDTC). Solution samples included Ag-malate (10 mM $AgNO_3$ and 100 mM malate, pH 5.5) and Ag-GSH (10 mM $AgNO_3$ and 100 mM GSH, pH 5.5, prepared in anoxia). Again, solution samples were mixed with 20-30% glycerol to prevent ice crystal formation during cooling.

Determination of nanoXRF detection limit

The detection limit for Ag in our conditions was estimated using a free of matrix AXO standard (AXO-RF8-200-S2453, 400 nm thickness). This reference does not contain Ag, so the fluorescence Kβ line of Pd was used as the closest element to Ag. Detection limit is defined as follows (Ekinci et al. 2013):

$$LOD = \frac{3\sqrt{B}}{I}C$$

Where I is the total intensity of the fluorescence peak (counts), B is the background (counts) and C is Pd concentration in the AXO. For the experimental conditions ($5.80 \cdot 10^9$ ph/s, 0.1s dwell time, 50 x 50nm pixel size), the detection limit was 0.34 ± 0.09 attograms per pixel (calculated on n = 20 pixels). which can be translated to 27 ± 7 mg L^{-1}.

Intracellular silver determined by ICP-AES after cell lysis

Cells grown in 250 mL Erlenmeyer flasks with or without nanoparticle stress were harvested by centrifugation at 8000 rpm for 30 min. The pellet (about 80 µL) was washed twice with 2 mL of PBS buffer and was resuspended in 225 µL of lysis solution containing 200 µL of TES buffer (10 mM Tris, 1 mM EDTA, 0.2 M sucrose), 20 µL of 30 mg mL-1 lysozyme, and 5 µL of 1/50 benzonase 5KU (Sigma, ref E1014) during 20 min at 37°C. The lysis supernatant was collected after centrifugation at 13000 rpm for 10 min. This lysis supernatant was digested before Ag determination by adding 5 mL ultrapure HNO3 at 65% heated at 180°C for 20 min in a microwave (Novawave, SCP Sciences). Samples were then diluted by addition of 10 mL ultrapure water. ICP-AES measurements were done using a Varian 720ES at ISTerre, using the Ag line at 328.068 nm. The efficiency of the digestion was tested on Ag-NPs, Ag2S-NPs and Ag lactate. The recovery was 75% Ag2S-NPs and total for Ag and Ag lactate.

Results

Size and morphology of the NPs

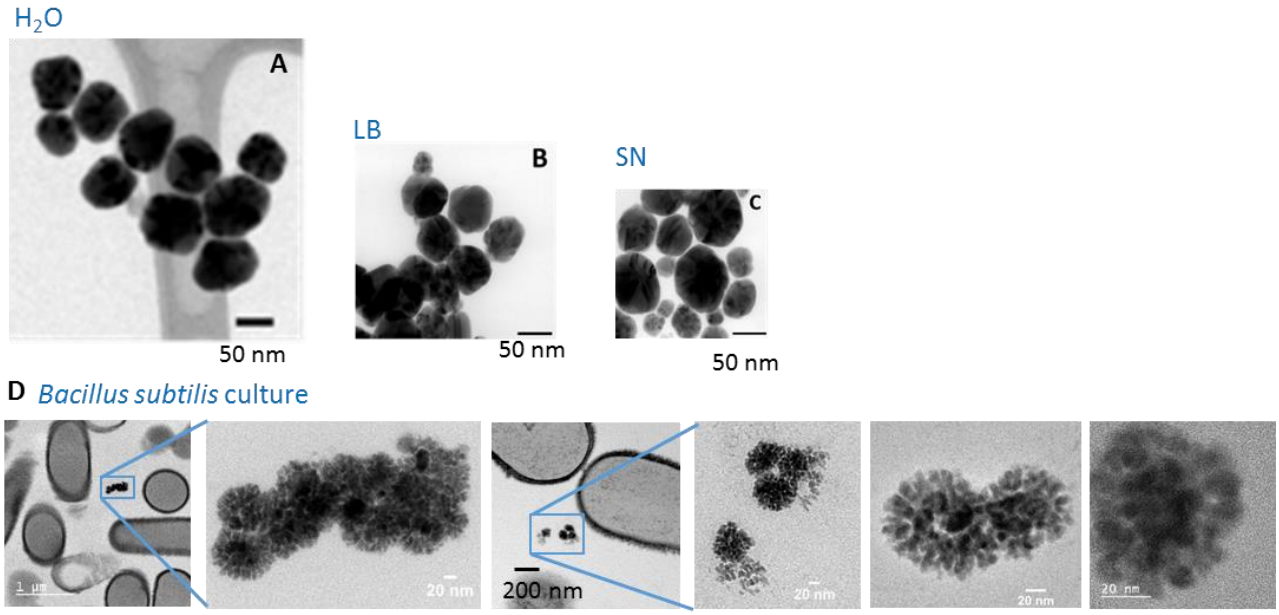

Figure S3: Morphology and particle size of Ag-NPs after incubation for 5 h in water, LB and SN (in NA conditions) (A, B, C, respectively), and with *B. subtilis* (D), observed by TEM.

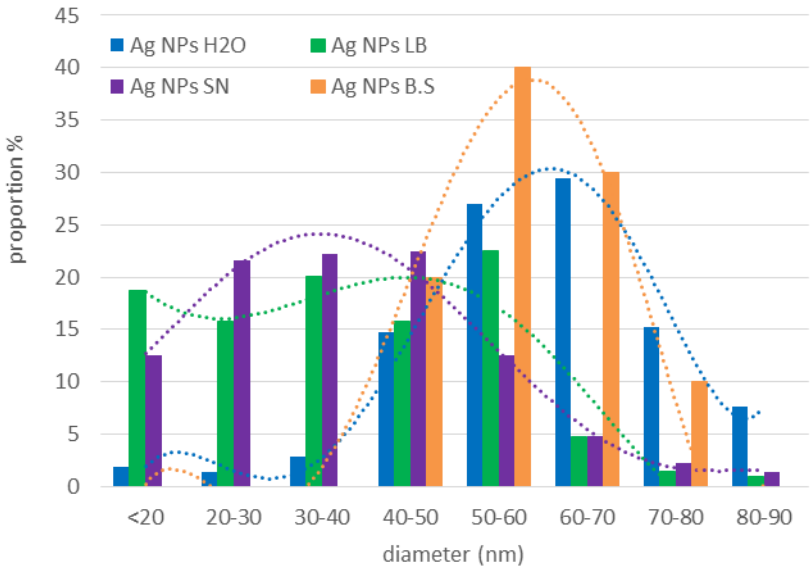

Figure S4: Particle size distribution of Ag-NPs after incubation for 5 h in water, LB and SN (in NA conditions), and with *B. subtilis*, derived from the TEM image analysis of about 200 nanoparticles for the H_2O, LB and SN conditions, and 20 nanoparticles for the bacterial culture.

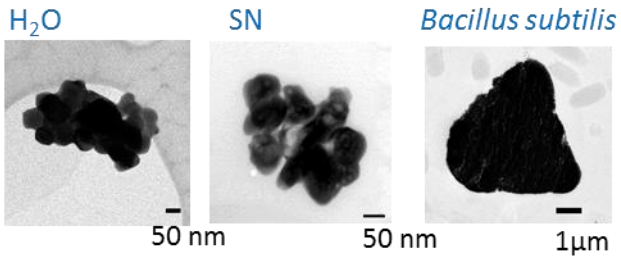

Figure S5: Morphology and particle size of Ag_2S-NPs after incubation for 5 h in water, SN (in NA conditions) and with *B. subtilis,* observed by TEM.

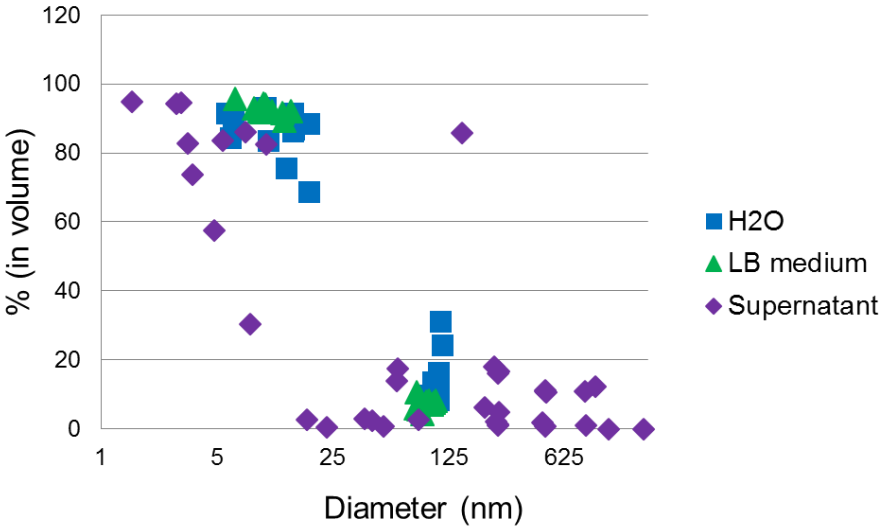

.

Figure S6: Dynamic light scattering (DLS) results for Ag-NPs after incubation for 5 h in water, LB and SN (in NA conditions). The diameter is represented in logarithmic scale.

TEM analyses

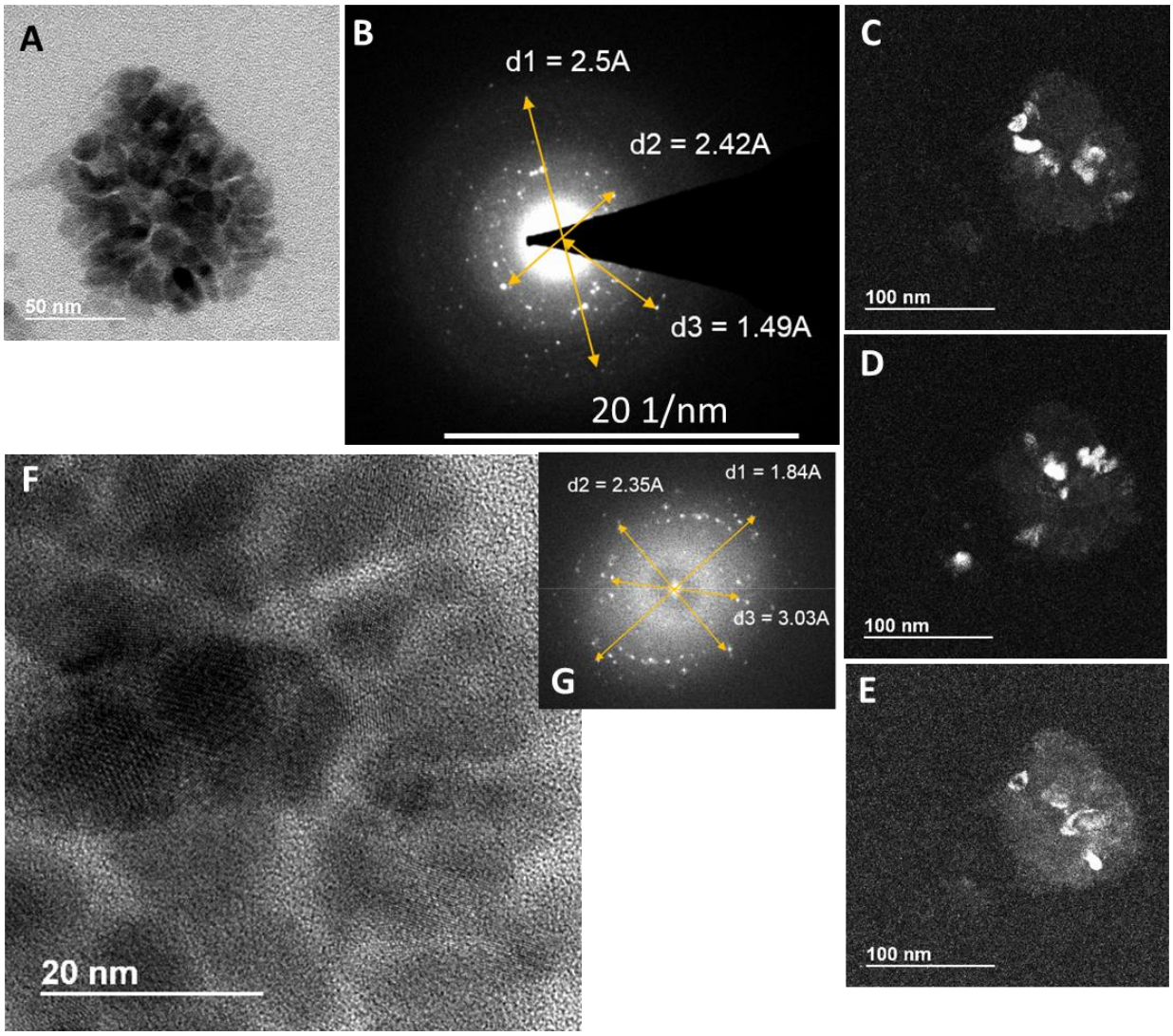

Figure S7 : Analyses of a representative aggregate of Ag-NPs after incubation with *B. subtilis*. A, TEM image of the aggregate. B, electron diffraction obtained on the aggregate. Measured distances of d1, d2 and d3 of 2.5, 2.42 and 1.49 Å, with d1-d2 and d2-d3 angles of 116.4° and 43° are consistent with acanthite structure. C-E: Dark field images obtained by selecting a group of 2-3 spots in the SAED image. F,G High resolution image (F) and its Fourier transform (G) of a region of the aggregate. Again, measured distances d1, d2 and d3 of 1.84, 2.35 and 3.03 Å, with d1-d2 and d2-d3 angles of 90° and 125° are consistent with acanthite structure.

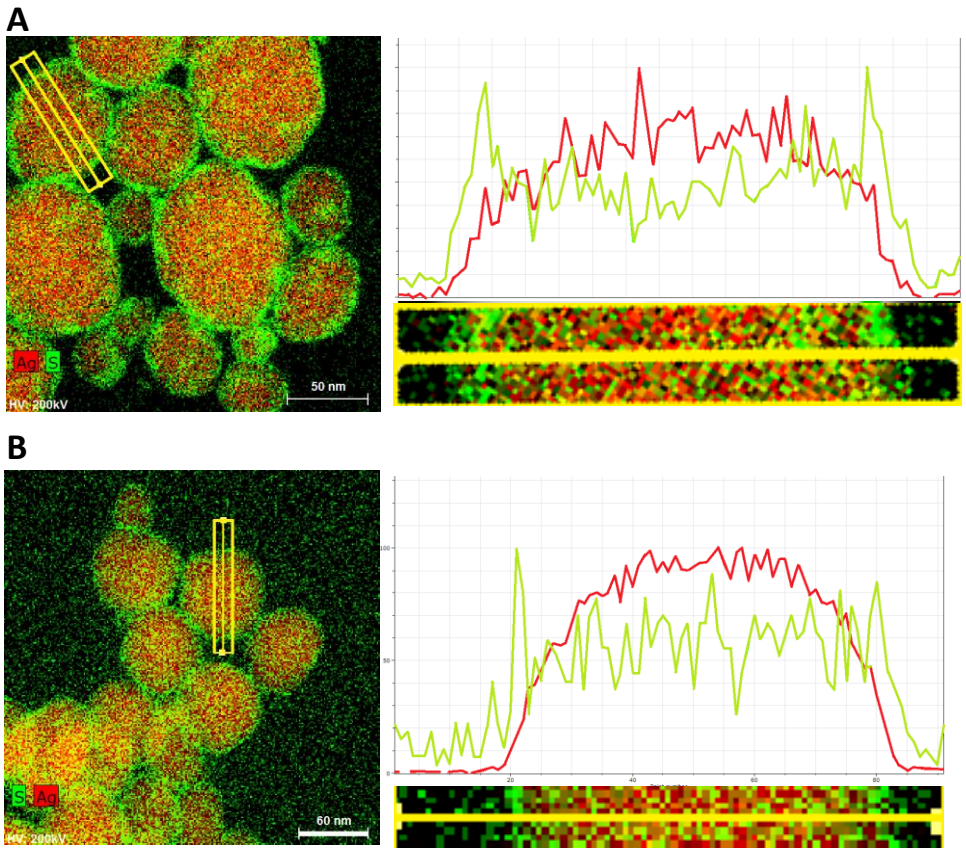

Figure S8: Example of elemental profiles for Ag (in red) and S (in green) across a Ag-NP after incubation in SN (A) and in LB medium (B), both in aerated condition. Data were extracted from the EDX maps. The S signal at the edge of the particle is stronger in SN than in LB, and for both conditions the highest S signal corresponds to a decreased Ag signal compared to the center of the particle.

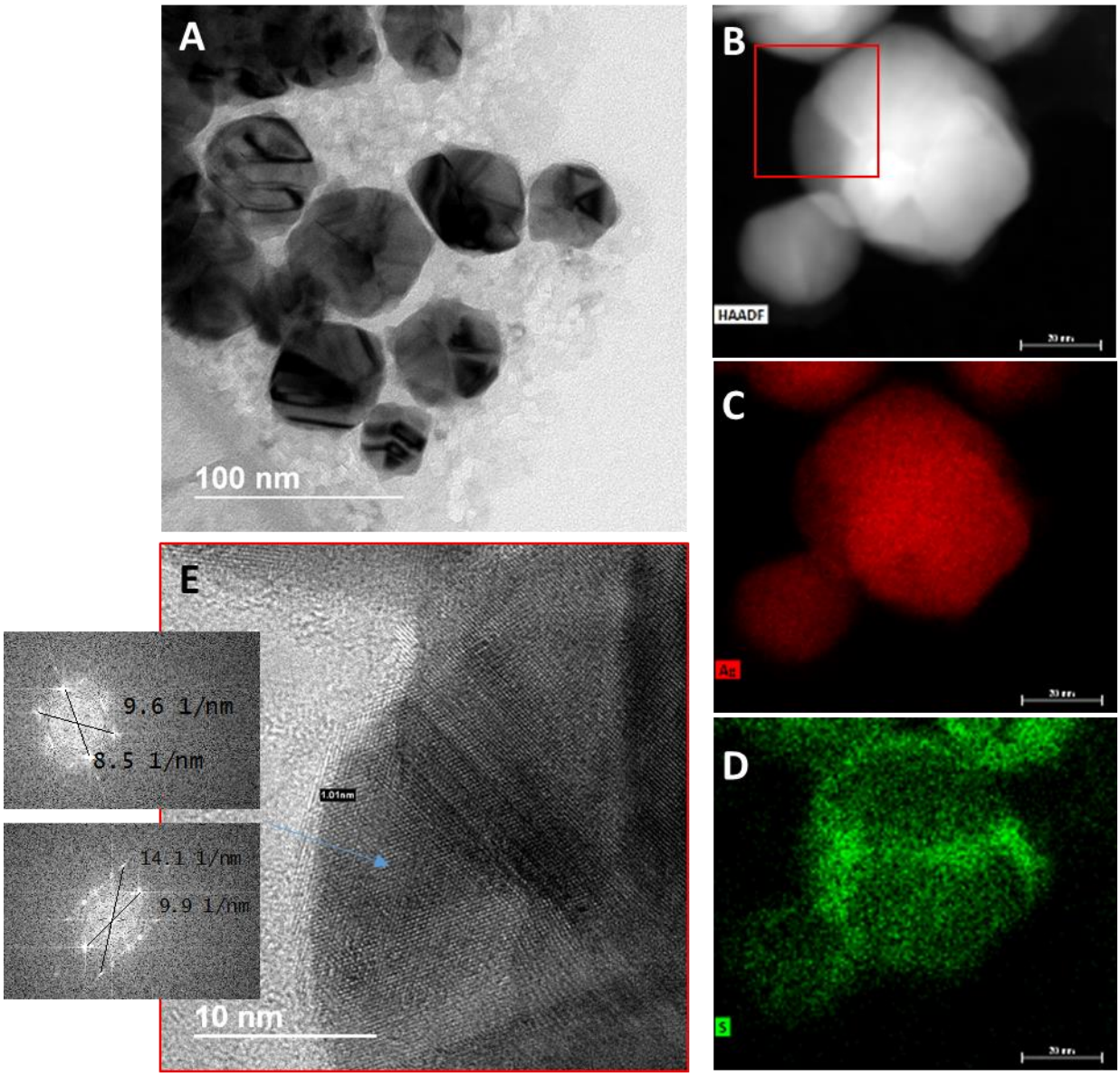

Figure S9: TEM observations of the Ag-NPs after incubation in SN, in aerated conditions. In A, the shades on the Ag-NPs indicate that the crystals are multi-twinned, with crystal dislocations appearing in dark or light gray. In addition, an organic matrix surrounding the NPs is visible. B, observation of two particles, and Ag (C) and S (D) elemental maps obtained by EDX. In this case, the sulfidation seems to progress near the crystal dislocations. E, High resolution image of the S-enriched zone (red square in B). The crystalline phase is Ag^0.

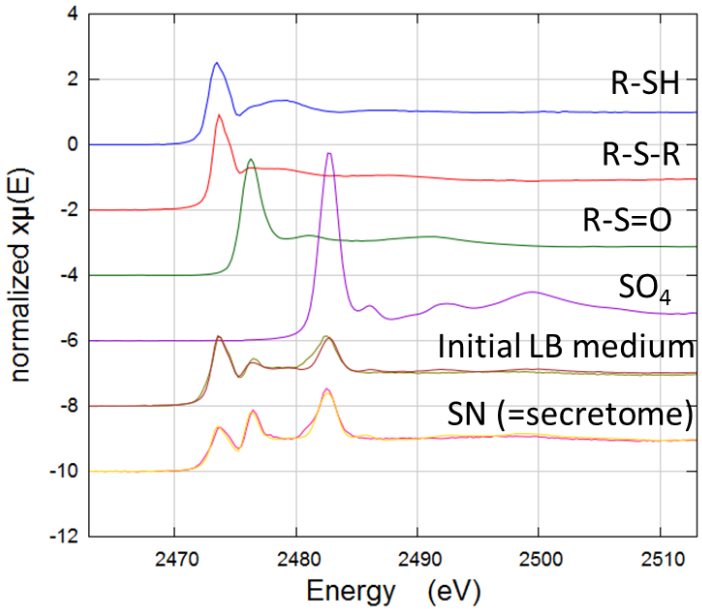

% of S species

R-SH	R-S-R	R-S=O	SO4	Sum	R factor
32	45	8	20	105	0.023
26	22	28	27	103	0.032

Figure S10: S K-edge XANES spectra for the LB initial medium and for the freeze dried supernatant of *B. subtilis* culture in stationary phase without silver. Spectra were recorded on beamline ID21 at the ESRF, and fitted by linear combination of reference compounds (brown and yellow spectra), as described previously (Sarret et al., 1999). The molar percentage of the sulfur species are presented in the figure.

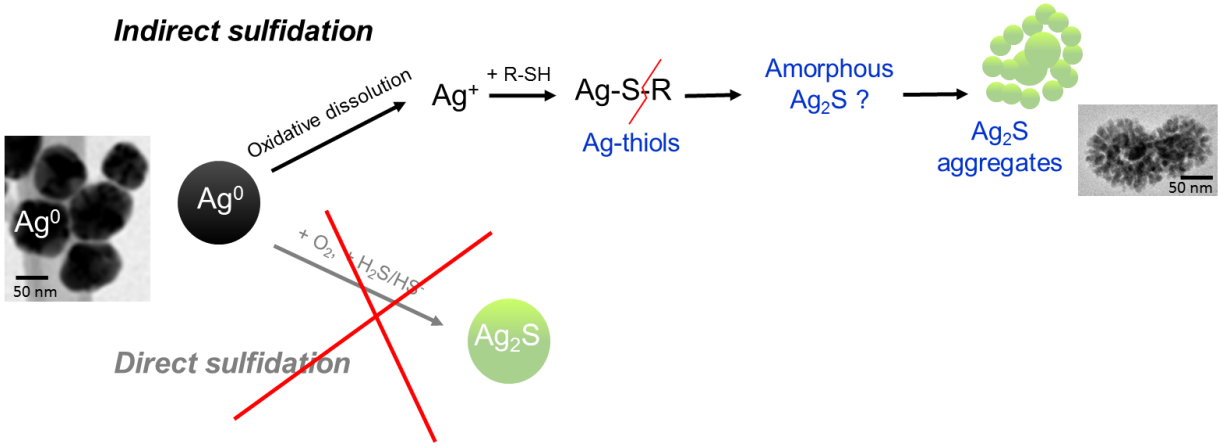

Figure S11: Proposed mechanism of sulfidation of Ag-NPs in the presence of *B. subtilis*.

References

Du, N.; Zhang, H.; Sun, H. Z.; Yang, D. R., Sonochemical synthesis of amorphous long silver sulfide nanowires. *Materials Letters* **2007,** *61* (1), 235-238.

Ekinci R, Ekinci N, Senemtasi E. 2013. Effect of Analysis Time on Detection Limit by Energy Dispersive X-Ray Fluorescence Spectrometry. Asian Journal of Chemistry 25: 2557.

Levard, C. *et al.* Sulfidation Processes of PVP-Coated Silver Nanoparticles in Aqueous Solution: Impact on Dissolution Rate. *Environ. Sci. Technol.* **45,** 5260–5266 (2011).

Sarret, G.; Connan, J.; Kasrai, M.; Bancroft, G. M.; Charrie-Duhaut, A.; Lemoine, S.; Adam, P.; Albrecht, P.; Eybert-Berard, L., Chemical forms of sulfur in geological and archeological asphaltenes from Middle East, France, and Spain determined by sulfur K- and L-edge X-ray absorption near-edge structure spectroscopy. Geochim. Cosmochim. Acta 1999, 63 (22), 3767-3779.